This is a repository copy of *Effect of grout properties on shear strength of column base connections: FEA and analytical approach*.

White Rose Research Online URL for this paper:
http://eprints.whiterose.ac.uk/120691/

Version: Accepted Version

EFFECT OF GROUT PROPERTIES ON SHEAR STRENGTH OF COLUMN BASE CONNECTIONS: FEA AND ANALYTICAL APPROACH

Mohamed A. Shaheen[1], Konstantinos Daniel Tsavdaridis[2*], Emad Salem[3]

[1]MSc, Civil Engineering, Al-Azhar University, Cairo, Egypt

[2] Associate Professor of Structural Engineering, Institute for Resilient Infrastructure, School of Civil Engineering, University of Leeds, LS2 9JT, Leeds, UK k.tsavdaridis@leeds.ac.uk

[3] Associate Professor of Structural Engineering, Department of Civil Engineering, Al-Azhar University, Cairo, Egypt

*Corresponding Author

ABSTRACT

Concrete grout is used in most column base connections to facilitate the construction process and to ensure that full contact is achieved between the steel plate and the concrete pedestal. However, insignificant attention has been given to its use and performance while there is a lack of clear understanding towards its contribution to the shear strength of column base connections. A comprehensive finite element (FE) study is presented herein investigating the shear capacity of the column base connection on the grout thickness and strength. 3D FE models incorporate important behavioural aspects including the surface interaction and multi-axial constitutive models of the assemblages. The results of the investigation indicated that the introduction of grout improves the behaviour and strength of the column base connections significantly by developing a different load path system consisted of the grout strut, the friction between the base plate and grout, and the tension in the anchor rod due to second order effects. It is found that the current design codes of practice do not consider the positive influence of grout and lead to very conservative shear strengths. Furthermore, the paper proposes a mathematical equation to account for the lateral displacement which is overlooked in the current international regulations.

Keywords: steel column bases; base plate; grout properties; grout strength; grout thickness; monotonic shear load; anchor rod; holding down bolt; parametric study; numerical approach

1. Introduction

It is accepted that the base plate is a critical component of the steel structures as it controls the initial stiffness of the frame. Frame stiffness is mainly controlled by the boundary conditions; while steel column bases are usually assumed as a simple connection or a rigid connection. The assemblage of an exposed column base plate connection includes the steel column, base plate, anchor rods, concrete footing and grout. The grout is used for the ease of the column's erection; the exposed part of the anchors can be adjusted during erection before pouring the grout. The grouting also ensures that full contact and compactness around this restricted space is achieved between the steel plate and the concrete pedestal (part of the concrete foundation that is placed after the concrete foundation hardened). Despite the extensive use of the grout in most base plate connections, it has received limited attention [1]. The need for further consideration is also supported by other publications [2,[3], in which it was highlighted that the understanding of shear transfer in exposed column base plates is limited, and there is yet a lack of research which investigates the shear failure of the connection.

In many studies [4-6], the effect of grout is neglected by not including it in the test and/or by placing the base plate in direct contact with the concrete pedestal (**Fig. 1b**). The exposed length and the bearing between the anchor and grout play a significant role in the ultimate strength of the connection as it is affecting the force developed in the anchor rod. For example, an anchor rod with differently exposed lengths loaded in double shear was tested by Zhibin et al. [4]. The study was carried out for a sole anchor and ignores the effect of the interaction between the assemblages of the connection; particularly the bearing between the anchor rod and grout. It was concluded that the exposed length affects significantly the capacity and the failure mode of the anchor rod. The failure mode of the anchor may be changed from shear fracture (in the case of short exposed length) to flexural-dominant or tension fracture when larger exposed length was used. Swirsky et al [5] investigated anchor rods loaded in shear with different diameters which have the same exposed length. Instead of concrete grout, elastomeric bearing pads were used between the loading plate and concrete surface (**Fig. 1c**). The tests showed that the anchor rod with the exposed length failed under combined loading (i.e. shear and bending). Furthermore, with the increase of the exposed length, the lateral deflection increased substantially whereas the shear strength reduced. Nakashima [6] conducted an experimental test for three 12mm and two 16mm anchors loaded in shear with different grout thicknesses. It was observed that with the increase of grout thickness, the capacity decreased, and the ultimate displacement increased. However, the decrease in the shear capacity of the anchor rod was not significant when different grout thicknesses were used. For instance, the ultimate shear reduced merely by 5% when grout thickness increased from 10mm to 40mm.
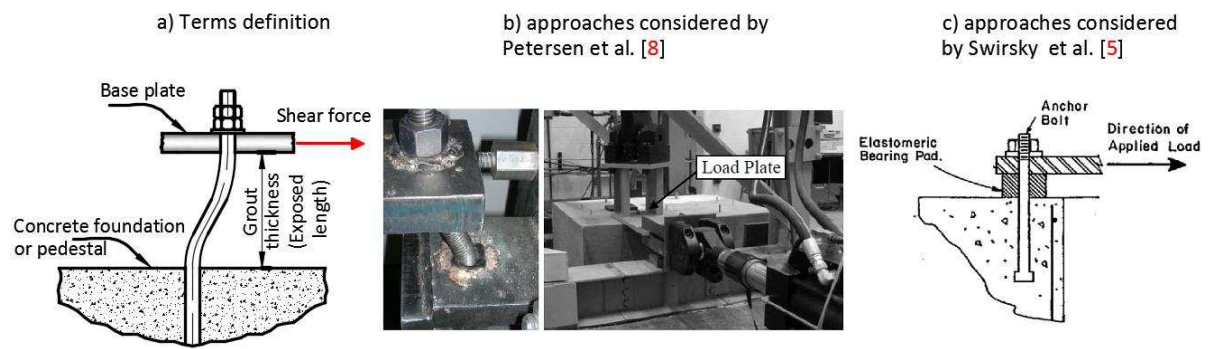
Fig. 1: Different approaches in previous researches

2. Current practice

2.1. Grout types

There are various grout types with diverse properties designed for different applications. However, the grout volume is the major characteristic that affects load transfer from column bases to the concrete pedestal to ensure complete and permanent filling of the space between the base plate and the footing. Plain grouts consist of cement, fine aggregates, and water may develop adequate strength. Shrinkage and bleeding of the plain grout may result in loss of contact with the base plate, hence, additives are utilized to maintain permanent contact with the base plate.

According to ACI 351.1R-99 [9], frequently used in practice grouts are the hydraulic cement grouts and the epoxy grouts. The former type has the same mixtures of plain grout (i.e., fine aggregate and water) with further additives to compensate for shrinkage (e.g., aluminium powder) or to prevent bleeding, and it is known as cementitious non-shrink grout. Non-shrink grouts are acceptable for most applications and have the capability to transfer static as well as dynamic and impact loads. In the current study, the cementitious non-shrink grout was considered.

2.2. Concrete strength and code references

It is well known that the strength of grout is influenced by many factors, such as the quality of raw materials, water/cement ratio, coarse/fine aggregate ratio, temperature and relative humidity. Inaccurate estimation of one or more of these factors inevitably leads to poor grout (or grout strength lower than the anticipated). Moreover, the bearing area between the base plate and the grout can be significantly affected by either grout leakage, inadequate mixing of grout, wrong placement method, or poor grout. In addition, it worth to note that the grout strength suggested by various country regulations is markedly different. For instance, the desired grout strength suggested by the AISC design guide [10] should be at least twice the strength of the concrete pedestal to transfer the load from the super-structure to the foundation safely. On the other hand, ACI 351.1R-99 [9] suggests the preferred strength with no regard to the strength of concrete pedestal as typical compressive strengths of grouts set between 35 and 55 MPa. EC3 and section 6.2.5 (7) [11] states that the characteristic strength of the grout should not be less than 0.2 times the characteristic strength of the concrete pedestal. The limit suggested by EC3 is exceptionally low while the value is based on experimental tests. It is still questionable whether these tests cover the most unfavourable cases [12]. The strength of non-shrink cementitious grout widely used in the construction industry is more conservative than the values suggested by the regulations. The most popular grout materials used in practice worldwide are ranging between 48 and 56 MPa as provided by grout suppliers [13 and [14].

2.3. Grout thickness

The minimum grout thickness depends significantly on the practicality of pouring concrete under the base plate. Therefore, the minimum thickness must be sufficient to place the grout in a realistic manner. In engineering practice (as provided by the manufacturers' guidelines [13 and [14] and design codes [9 and [15]), the minimum preferred grout thickness is 25mm. ACI 351.1R-99 requires a minimum thickness of 25mm for flow-able hydraulic cement grout placed by gravity. When the flow length is larger than 300mm, the thickness should be increased by 13mm for each additional 300mm to a maximum of 100mm.

3. Purpose of the study

Despite the plethora of inaccuracies found in engineering practices, various grout strengths suggested by different regulations. This leads to the conclusion that the effect of grout strength and thickness on the behaviour of base-plate received no much attention. In this paper, the shear resistance of base plate connections is studied with respect to grout properties via comprehensive numerical finite element (FE) analyses that are validated against experimental results found in the literature. Different grout strengths ranging from poor (5.6MPa) to high grout strength (50MPa) are considered. The thicknesses are selected based on the most common ones found in engineering practice (ranging from 25mm to 100mm). To understand the effect of the grout thickness, a column base connection is examined when grout layer omitted (i.e., with sole anchor rod) and compared with the ones including the grout layer. An advanced three-dimensional (3D) nonlinear FE model is developed through the use of general-purpose FE software package ABAQUS v6.10 [16].

4. Finite element modelling

4.1. Description of the finite element model

A 3D FE model was employed using solid elements to model the base plate connection. The experimental specimen (#M1) as tested by Gomez et al. [17], was utilised to validate the current FE model. **Fig. 2** illustrates the detailed configuration and parameters that represent the test apparatus. Only half of the specimen was modelled in FEA due to the symmetry of the geometry and loading (i.e., around the web of the column) as it is shown in **Fig. 3**. The diameter of anchor rods was 19mm (0.75in) extended from the bottom of the anchor to the top of the concrete pedestal, and the rest of the length was threaded. To model the threaded part in ABAQUS, the anchor rods were modelled in two parts with different diameters. The lower part of the entire anchor was 19mm and ends at the top of the pedestal's surface, while the upper part of the anchor (net diameter) was 16.3mm (as it was measured by Gomez et al. [17]). Both geometric and material nonlinearity was introduced during the analysis and the numerical results obtained were compared with the experimental ones.
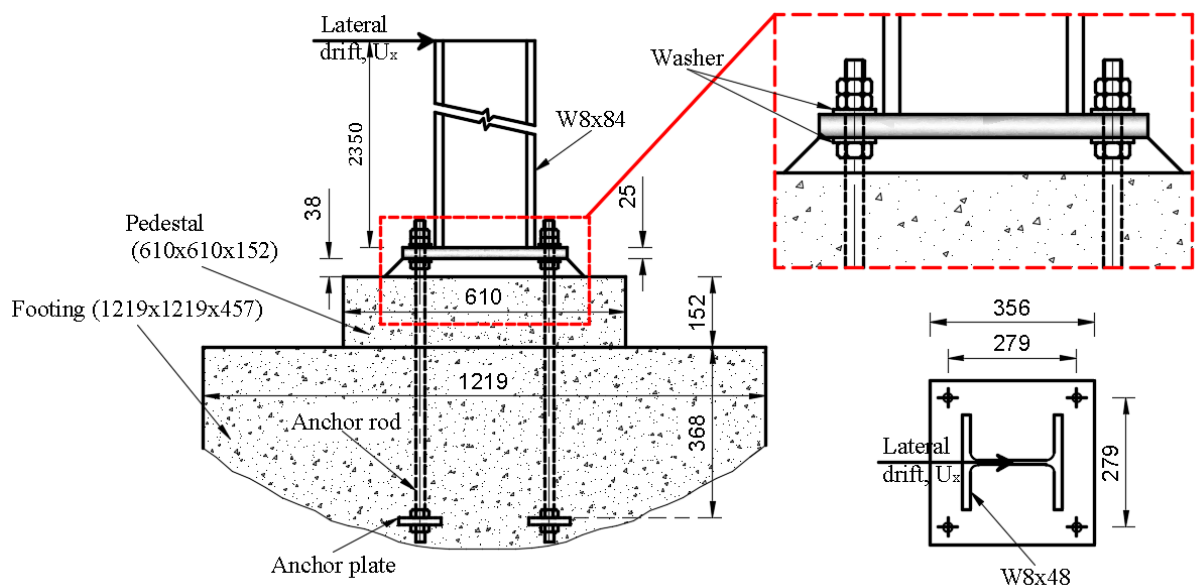

Fig. 2: Geometry of the specimen (mm)
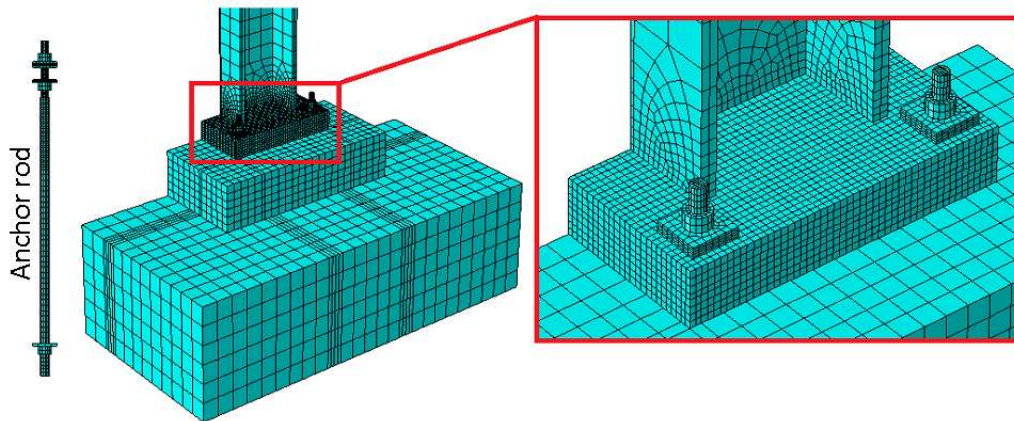
4.2. Element types and contact conditions

The connection components (i.e., grout, pedestal footing, base plate, anchor rods, washers, nuts, anchor plate and column) were modelled using 8-node linear brick elements reduced integration (C3D8R). The large dimensions of the experimental specimen required an equally large number of elements to obtain acceptable results. Instead of that a complex mesh plan was assigned to the parts considering that the region where high-stress concentrations were expected the mesh was refined to provide more accurate results, as it is illustrated in **Fig. 3**. For example, the parts of the anchor rods in contact with the base plate and grout had a very fine mesh to avoid the convergence problems due to high-stress concentration particularly under shear loading (e.g., hourglass effect).
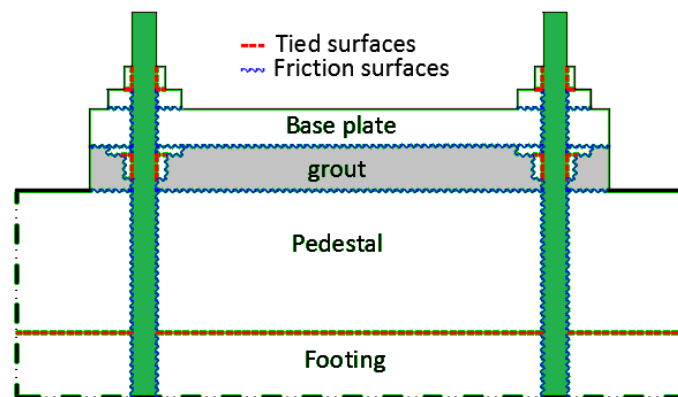

Fig. 4: Assigned contact surface

The contact and gaping under applied load between the base plate and grout in the tension side as well as the anchor rod and concrete have to be considered carefully as they affect the performance of the connection significantly. The surface between the parts where no gapping is expected, such as the pedestal and concrete footing, are simulated as monolithic (i.e., tied surfaces in ABAQUS). It was also decided that a tie constraint could be defined between the column and the base plate while the weld was designed in such a way that it will not fail during the experimental test (PJP weld with reinforcing fillet weld - the total thickness of the weld was 25% larger than the flange thickness). Similarly, the surfaces between anchor rods and nuts were also defined as tie constraints (**Fig. 4**).

The bond between the anchor rod and the concrete may fail at an early stage of the load application. It is therefore assumed that from the onset of loading the tensile force resisted by

the anchor plate and the bond can be neglected [12,[18,[19]. As a consequence of this, and further suggestions used in previous experimental studies, the anchor rod-concrete bond was ignored during the analysis. This accounts for the mechanism following the initial failure of the bond, evaluating the force resisted by the bearing between the steel elements and the concrete. Similarly, based on experimental observations [17], the bond between the grout and pedestal is damaged and the grout is completely separated from the concrete pedestal at an early stage. Consequently, the bond between grout and footing was neglected from the onset of the analysis and a friction surface was defined instead. **Fig. 4** demonstrates the defined friction and tie surfaces between the components of the connection. Surface-to-surface contact elements were assigned to the interface of the anchor rod and the concrete: (a) between the bottom surface of the base plate and the top surface of the concrete grout, (b) between the bottom surface of grout and pedestal, and (c) between the anchor rod and the base plate and washers. The tangential behaviour (i.e., the relationship between two contact surfaces in tangential direction) of the contact interaction was defined as friction using contact properties with a friction coefficient equal to 0.45 as suggested by Gomez et al.[17].

To resemble the experimental test, the FE model was monotonically loaded with the displacement control method up to 10.6% column drift (i.e., the length of the column divided by the maximum lateral displacement). Given that the length of the column was 2,350mm from the top of the base plate, the applied lateral displacement in the model was 249mm in the direction of its major axis. The descending post-plastic curve was not recorded during the experimental test as the 250mm was the stroke limit of the actuator. No axial load was considered during the experimental test and accordingly in the FE analysis.
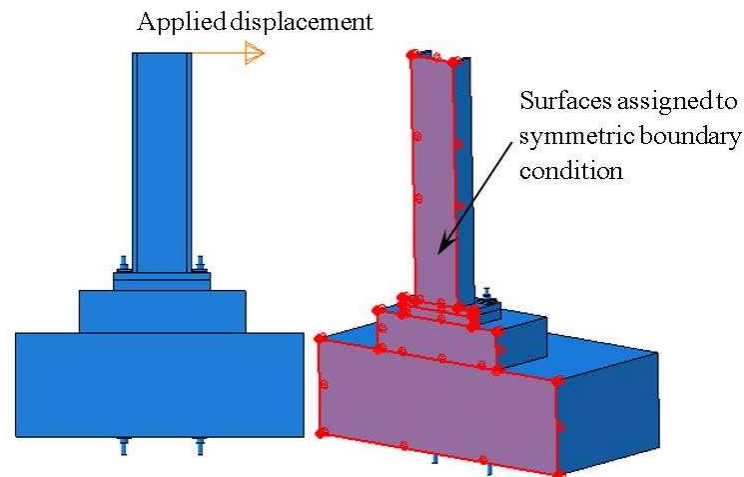

Fig. 5: Boundary conditions and applied force

As it was aforementioned, half of the tested specimen was modelled considering the axis of symmetry passes through the centre of the column web. Therefore, symmetry boundary conditions were assigned at the centre of the model to simulate the behaviour of the full model as shown in **Fig. 5**. The movement of the bottom surface of the foundation was prevented in all three directions to simulate the experimental test.

4.3. Material modelling

A nonlinear material obeying the von Mises yield criterion and isotropic hardening was used to model the anchor rod and base plate. The definition of steel material in ABAQUS requires the true stress and plastic strain values. The required values were calculated based on ancillary experiments on material coupons carried out by Gomez et al. [17] as it is shown in

Fig. 6 and **Fig. 7** for the anchor rod and base plate, respectively. The material properties of the anchor rod in elastic range were: Young's Modulus E=203GPa, ultimate stress f_u=1010MPa, and yield stress f_y=785MPa. During the experimental test, a large column section was employed to maintain the elastic range and avoid local buckling. Consequently, the modulus of elasticity (E=218GPa) and Poisson's ratio (0.3) were only defined in the FE model for the column. The washers, nuts and, anchor plate were modelled with an elastic-perfectly-plastic material with modulus of elasticity 200GPa and yield stress 350MPa.
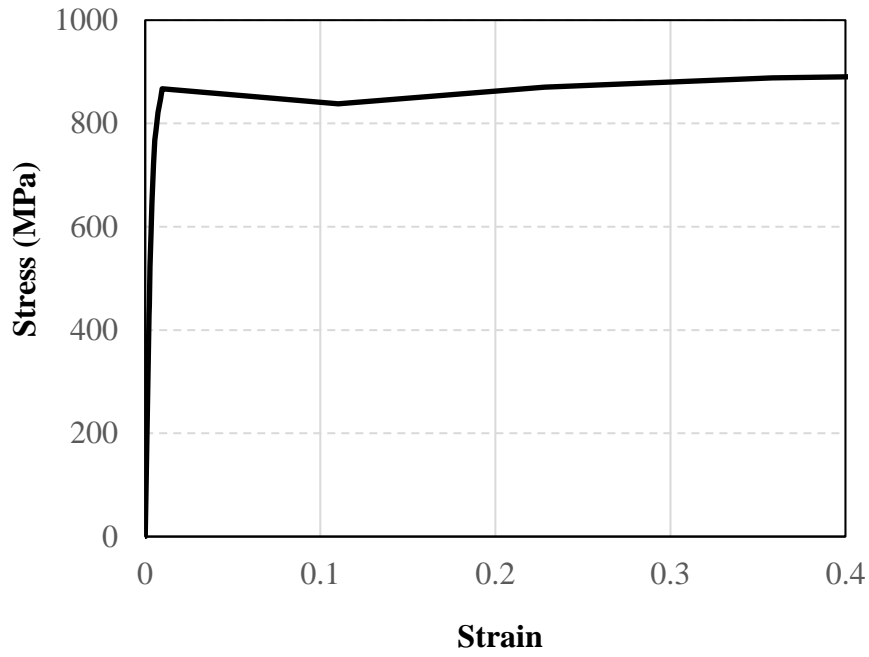

**Fig. 6:** Stress-Strain curve for anchor rod as tested by [17]
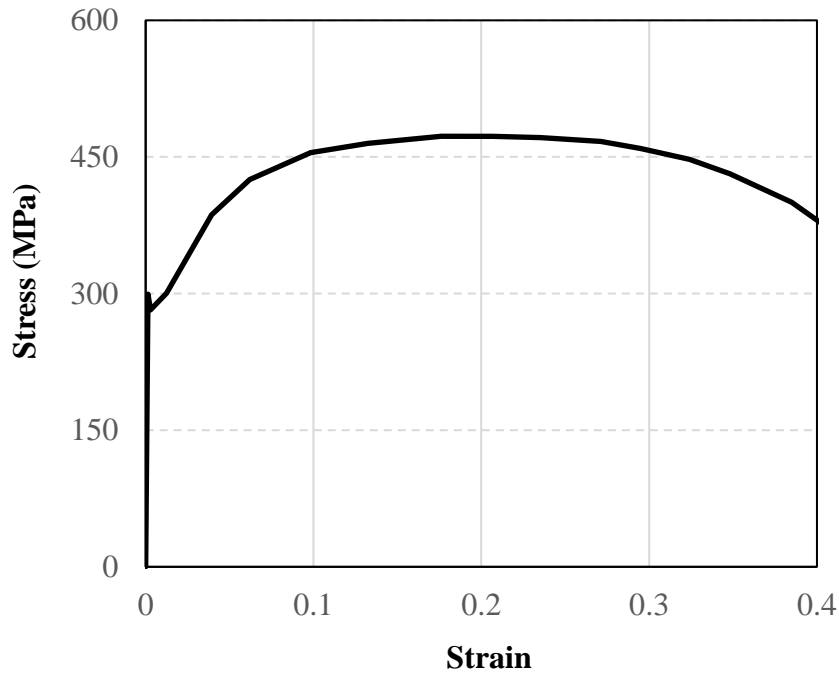
Fig. 7: Stress-Strain curve for base plate as tested by [17]

The concrete pedestal and foundation were defined as an elastic material since no significant plastic response was captured in the experimental test [17]. On the other hand, the grout was modelled employing the damage plasticity approach. Nominal concrete material properties are required to model both the elastic and plastic behaviour in compression and tension including strain softening and tension stiffening. A constitutive law for the concrete under compression was employed based on the experimentally verified numerical method by Hsu and Hsu [20]. This approach was used to derive the stress and the corresponding strain up to $(0.3\sigma_{cu})$ in the descending branch of the stress-strain curve by using only the maximum compressive strength σ_{cu}. **Fig. 8** defines the parameters used in the following equations: the concrete compressive strength (σ_{cu}), strain corresponding to concrete compressive strength (ε_0), and the maximum strain corresponding to $(0.3\sigma_{cu})$ in the descending part (ε_d). **Fig. 9** shows the compressive stress-strain curve of the concrete grout.
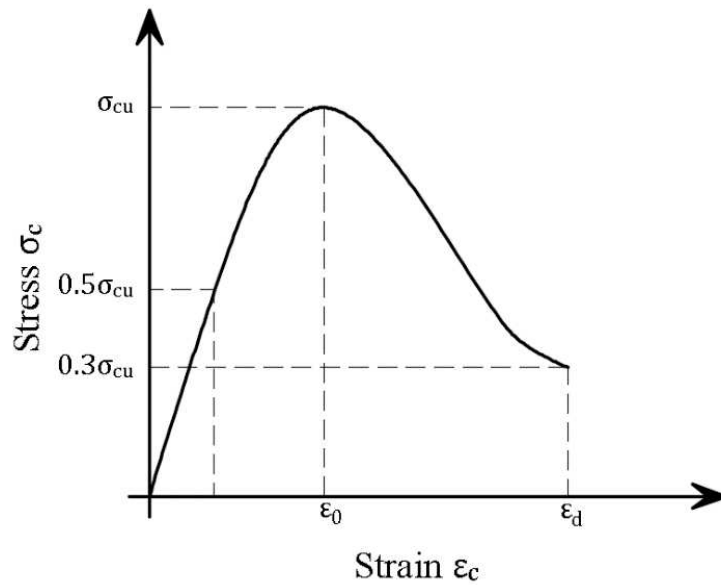
Fig. 8: Compressive Stress-Strain Relationship as proposed by [20]
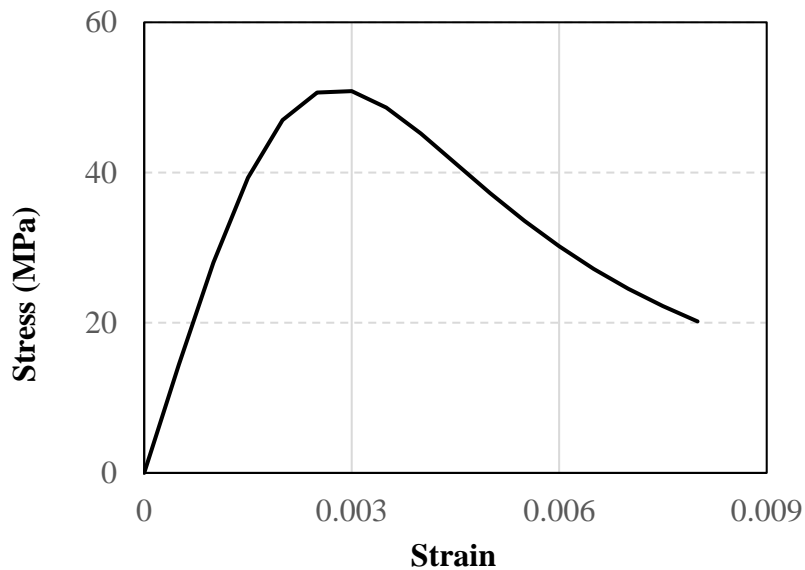
**Fig. 9:** Compressive stress-strain for concrete grout

The tension softening curve was developed using **Eq. (1)**, as it was proposed by Hilleborg [21]. This equation provides the relationship between the tensile stress of the

concrete (σ) and the crack width (w). The fracture energy of concrete (G_f) assumed to be 80N/m while the value of the concrete tensile strength (f_t) is calculated based on EC2 [22]. The relationship between the tensile stress and the crack width is shown in **Fig. 10**.

$$\sigma(w) = f_t(1 + 0.5\frac{f_t}{G_f}w)^{-3}$$

(1)
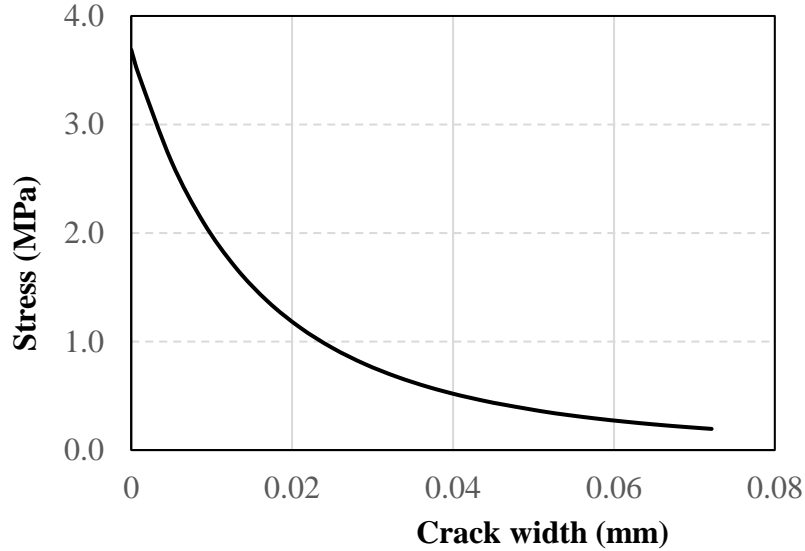
Fig. 10: Tensile stress-crack width for concrete grout

In certain cases, the use of concrete material, which exhibits softening behaviour and stiffness degradation, leads to severe convergence difficulties. A common technique to overcome the problem is to employ a viscosity parameter (μ). By using small values of viscosity parameters, it usually improves the rate of convergence of the model without altering the results [23]. It is necessary to examine different values of viscosity parameters to monitor its influence and wisely choose the suitable minimum value of the viscosity parameter [24]. The viscosity value was decreased until there were no significant changes in the results between any two successive FE models. The value of 0.001 was considered appropriate for further use. Default values were used for the other parameters to define the concrete damage plasticity model as it is illustrated in **Table 1**.

**Table 1**: Parameters of concrete damage plasticity model

ψ	ϵ	σ_{b0}/σ_{c0}	K_c	μ
35	0.1	1.16	0.667	0.001

Where: ϵ is flow potential eccentricity; σ_{b0}/σ_{c0} is the ratio of initial equibiaxial compressive yield stress to initial uniaxial compressive yield stress; K_c is the ratio of the second stress invariant on the tensile meridian to that on the compressive meridian.

5. Verification of the FE model

The comparison of the load-lateral displacement behaviours between the FE model and the experimental test data carried out by Gomez et al. [17] was recorded at the top of the column and it is shown in **Fig. 11**. The maximum applied load recorded during the experimental test was 53.4kN while the corresponding numerical result of the FE model was 55.5kN, which is higher by only 4%. The comparison of the load-displacement curves demonstrates the accuracy of the results. It is worth to note that the dips shown in the

9

1 experimental test curve were due to load relaxation as the test was paused to allow for visual
2 observations, however, this practice has not affected the results.
3
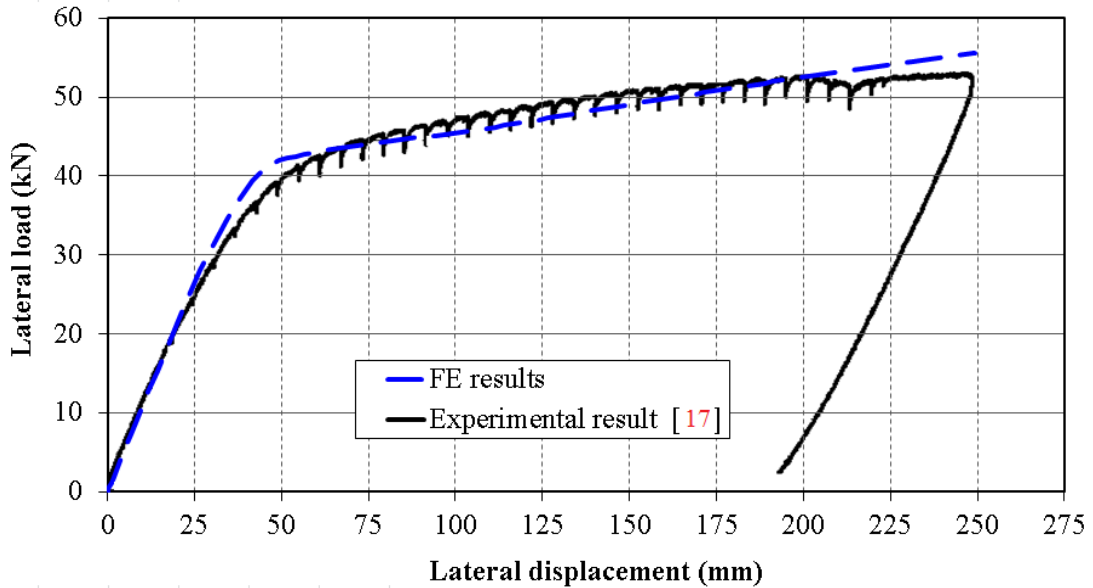
4
5 **Fig. 11:** Comparison of load-lateral displacement behaviours

6   Furthermore, the local behaviour of the assemblages was compared to the experimental
7 test in order to verify the actual response of the connection was modelled accurately. For
8 example, the average force in anchor rod, as well as the cracks and concrete crushing of the
9 grout, were compared to the test results as it is shown in **Fig. 12** and **Fig. 13**, respectively.
10 The comparison of the average rod force-column drift in **Fig. 12** depicts that the FE model
11 captured similar behaviour to the experimental test up to column drift 8% while there was a
12 slight difference beyond that drift level.
13
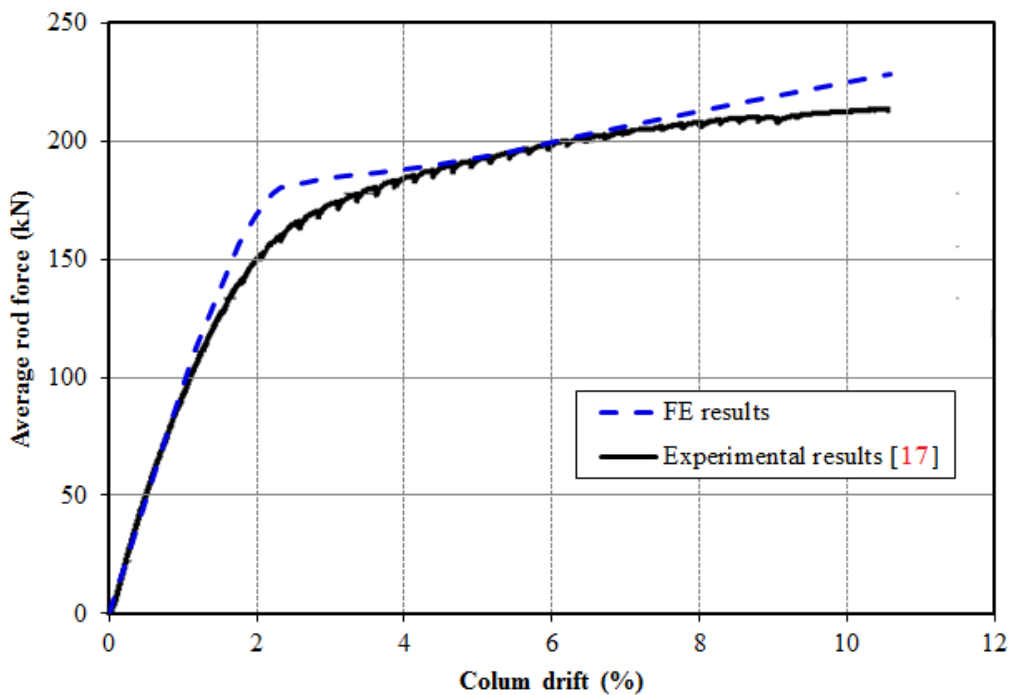
14
15 **Fig. 12:** Comparison of average rod force-column drift

Due to the MTS Series-244 220-kip actuator strok length capacity of 250mm, the test stopped before the anchor rod rapture, or the concrete failure took place. Grout damage was observed during the test at a drift ratio about 6%. The grout spalling was initiated at the extreme compression edge of the connection. The scalar stiffness degradation variable (SDEG) in ABAQUS was used to compare the damage of the grout with the experimental test. SDEG measures the residual stiffness of an element and takes a value from zero (undamaged material) to one (fully damaged material). In the case of concrete, the SDEG takes into account the damage due to tension (cracking) and compression (crushing). There was no documented picture for the grout damage at compression side found in the literature to compare it with FE model results. However, **Fig. 13** illustrates: (a) the grout damage at 6%, (b) the damage at the end of the analysis, and (c) the tension crack. As it is shown in **Fig. 13**, the grout spalling phenomenon was captured in the FE modelling as it was described in the literature.


a) Grout damage at 6% drift   b) Final grout damage   c) Crack in grout
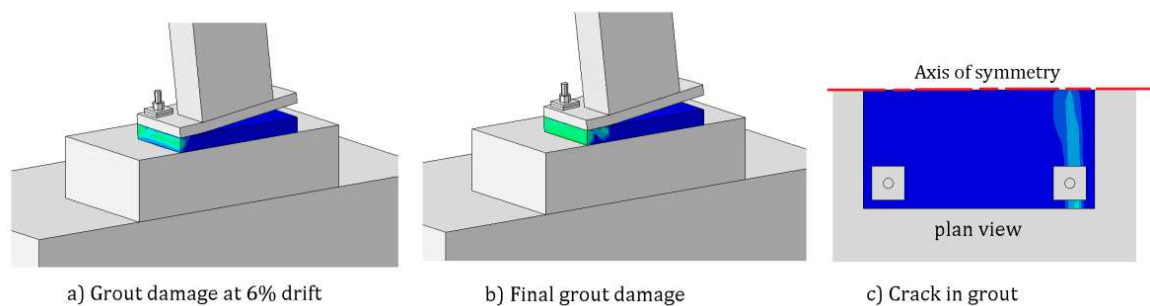
Fig. 13: Grout damage

6. Parameters and assumptions

The experimental specimen was designed to investigate the flexural behaviour of base-plate connections, and the same configuration and geometry were also used to study the behaviour of the connection under shear force. Throughout the parametric study, the force applied at the level of the base plate is representing a pure shear force acting on the connection. Also, to ease the erection, SCI/BCSA [15] recommends that the anchor rod should be positioned outside the column section, as it is designed in this specimen.

Two column base plate connections series were considered herein. The first series was column base connections with sole anchor rods (i.e., the grout layer was omitted from the analysis). As it was aforementioned, the purpose of these connections is to find out the shear capacity of the connection without grout and compare it when grout was also modelled. In this series, each specimen was represented by a one-field identifier. For example, E25 and E80 are the connections with exposed length of anchor rod 25mm and 80mm, respectively. The second series consisted of connections including the grout layer during the analysis. Each specimen was represented by a two-field identifier. For example, T25_S50 is the connection with grout thickness of 25mm and grout strength of 50MPa while in T60_S6 the grout thickness was 60mm and strength was 6MPa.

The lateral displacement was applied at the level of the base plate. To avoid the stress concentration in the vicinity of the applied load, the force was applied to a reference point which was tied to the side of the base plate as it is shown in **Fig. 14**. The connections were subjected to ample displacement so that the ultimate shear strength can be recorded. As it was anticipated, the connection suffered large lateral displacements; both geometric and material non-linearity were considered during the parametric analysis.
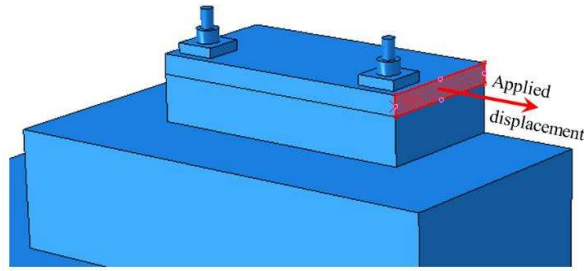
Fig. 14: Applied shear displacement

7. Shear capacity of the connection

Fig. 15 depicts the comparison between the load-displacement curve of four FE models with different grout thicknesses and the same models without the concrete grout. Similar to what it was observed in the previous studies [5,6,8,26], the initial stiffness of the sole anchor rod decreased as the exposed length increased. The grout acts as lateral support for the anchor rods under shear forces. This led to the connection with the grout have similar initial stiffness and independent of the grout thickness. With the increase of shear load, anchor rods experienced lack of confinement due to crushing of the grout. Beyond the elastic range of the connection, the strain hardening and peak lateral displacement depended significantly on the grout thickness. Overall, the shear strength of the connection decreased with the increase of the grout thickness. However, this decrease was not substantial as the capacity was decreased by approximately 10% when the grout thickness doubled from 25mm to 50mm.

In the case of the base plate being directly rested on the concrete pedestal, the connection exhibited shear-dominant behaviour. There was an obvious shear deformation with sudden failure based on the load–displacement curve. The connections with grout presented a different behaviour. As it is illustrated by **Fig. 15**, greater lateral deformation and strength degradation indicates that the bending failure of the anchor rod became predominant and led to flexural-dominant deformation. This was attributed to the damage of the grout in the vicinity of the anchor rod which eventually resulted in a large exposed portion. In addition to this, the large reduction in the cross-sectional area of the anchor rod may be one of the reasons affected the load capacity degradation.
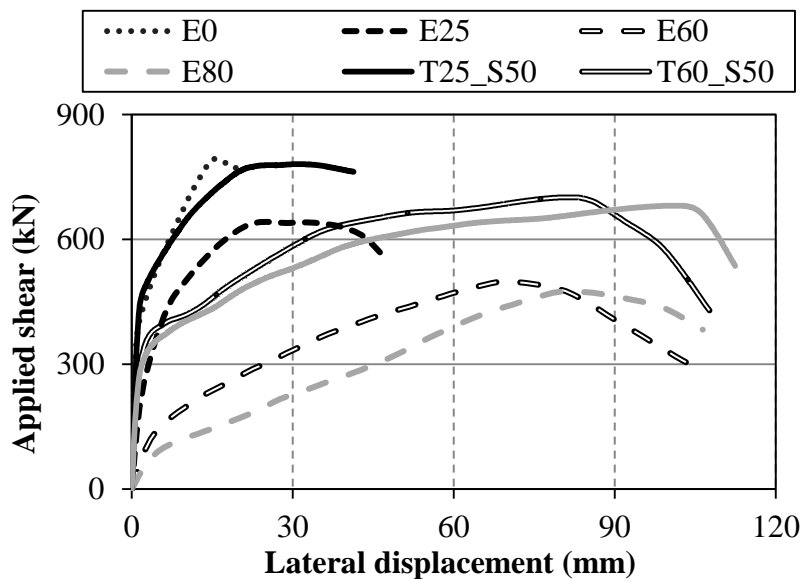
Fig. 15: Load-displacement for connection with and without grout

1   The shear capacities obtained from the FE analysis for the connection with a sole anchor
2   rod (in solid triangles) and connection with grout strength of 50MPa (in solid diamond) were
3   plotted against the shear values obtained from the literature in **Fig. 16.** The exposed length is
4   the distance between the top surfaces of the concrete pedestal to the bottom surface of the
5   base plate (i.e., equal to the thickness of the grout pad). To establish a comparison, the
6   recorded shear capacities were normalized by the code specified anchor shear strength equal
7   to $0.6A_r f_u$; where A_r is the effective sectional area of the rod and f_u is its ultimate tensile
8   strength. The collected data were conducted on a single anchor while a group of four anchor
9   rods were used in this study. In this way, the shear capacity of the connection was divided by
10   the number of anchors to get the average rod shear force.
11
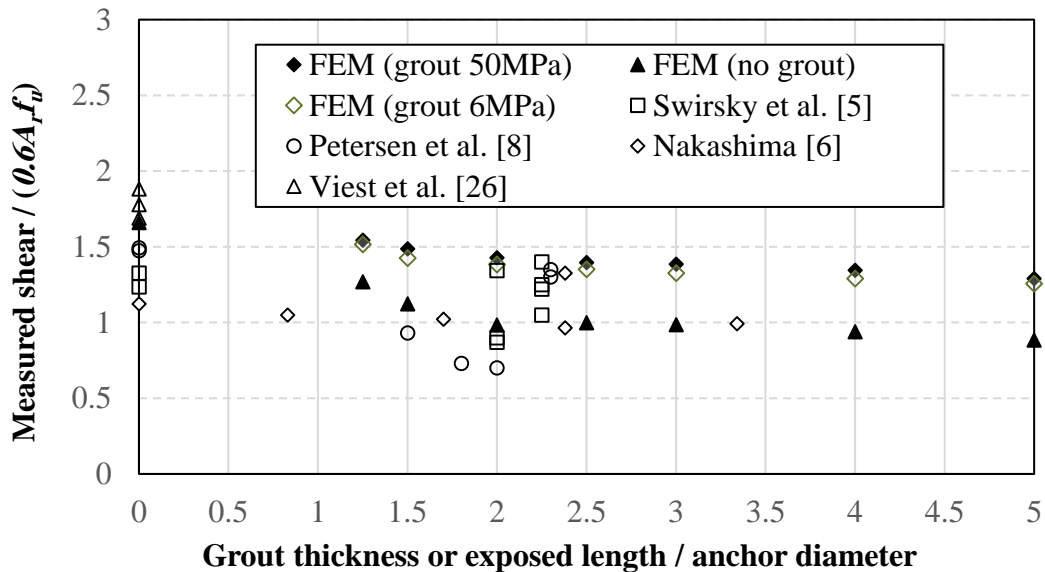
12
13   **Fig. 16:** Comparison between the shear capacity obtained from the FE model and
14   experimental tests
15

16   The sole anchor capacity obtained from FE analysis is approximately equal to the
17   average values recorded from the available tests found in the literature and agree well with
18   the experimental test carried out by Nakashima [6]. The friction and the interaction between
19   the connection components such as bearing between the anchor rods and grout, and friction
20   between the grout and base plate were ignored in the available experimental tests. Taking
21   these parameters into account by including the grout in the analysis, it is found that the shear
22   capacity increased significantly by approximately 20% and 40% when thin and thick grout
23   thickness was used, respectively. These results revealed that the positive influence of grout
24   should be taken into account during the design of column bases. Based on the comparison
25   between the connection with grout strength of 50MPa and the minimum strength value
26   suggested by EC3 [11] as 6MPa, it is clear that the grout strength has low effect on the shear
27   capacity of the connection. For example, the shear capacity was decreased by merely 4%
28   when the grout thickness was 80mm.
29

30   **8.   Importance of the concrete grout**
31   Concrete grout enhances the shear capacity of the connection because of two major
32   important factors. It was observed that within the elastic range of the connection, a concrete
33   strut was formed in the grout layer as shown in **Fig. 17a**. The formed strut affected the
34   connection behaviour significantly. The concrete strut restrained the anchor rod laterally. The
35   left anchor was supported by the grout in-between the anchors while the right anchor was

13

supported by the grout right to the anchor as shown by the stress contour. This lateral restraint led to the initial stiffness to be approximately independent of the grout thickness and matched with the connection where the base plate was in direct contact with the concrete pedestal. Therefore, within the elastic range of the connection, the anchor rod with different grout thicknesses behave similarly to having its exposed length equal to zero. As the load increase, the right anchor lost its grout support (black stress contour in **Fig. 17b**) which resulted in the degradation of the connection stiffness. However, due to the friction between the assemblages, two shorter struts formed instead, which improved the connection shear capacity. The second factor was the friction that developed between the base plate and the grout pad. Although there was no axial compression load applied in the FE models, a friction surface of the base plate and the grout pad was stemmed from the rotation of the front side of the base plate as a result of the unequal distribution of forces developed in anchor rods. The horizontal displacement (under applied load) leading to the increase of tension in the anchor rod (second order tension) due to the second order effect. Clamping action developed due to the vertical component of the increasing tension force was resulted in an extra contribution to the forces transferred by the friction.

From **Fig. 17b**, it is obvious that the right anchor resists less shear as it lost its lateral grout support. This was confirmed by the FE analysis. However, the distribution of shear force on anchor rods is not included in this manuscript as it deems lots of in-depth explanations and may considered as a separate study which requires further analyses.
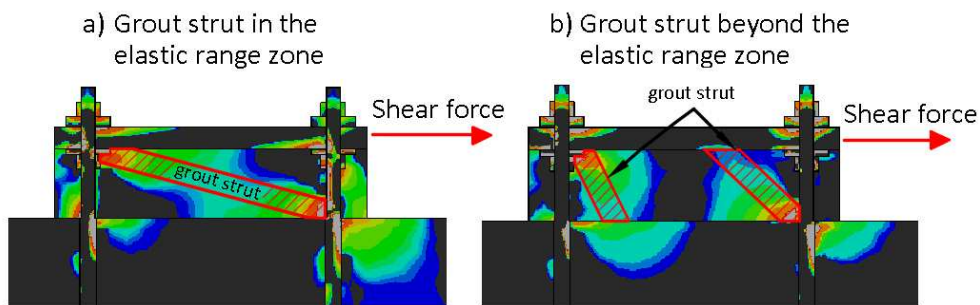
Fig. 17: Typical concrete strut (plot compressive stress)

In the case of connections without grout, the applied load was resisted by bending and shear forces in the sole anchor rods from the onset of the load application. The capacity of the connection was achieved by developing the plastic hinges in the anchor rods which was followed by the failure mechanism of the connection as illustrated in **Fig. 18a**. The number of plastic hinges increased in case of connection with grout which allow the force to be redistributed before the failure took place. The internal forces can be modelled by the so-called strut-and-tie model which is commonly used in reinforced concrete structures. The anchor rods serving as tension ties while compression strut can be represented by concrete grout. The redistribution of the forces caused the second order tension developed in the anchor rods for the connection with grout to be considerably higher than the values captured for peer connections with sole anchor rods, as it was illustrated in **Fig. 19**. The second order tension is overlooked in the design of anchor rod by the two cited regulations (ACI [28] and EC3 [11]). However, the results revealed that the above codes of practice should be revisited and the second order effects should be considered in the design process.
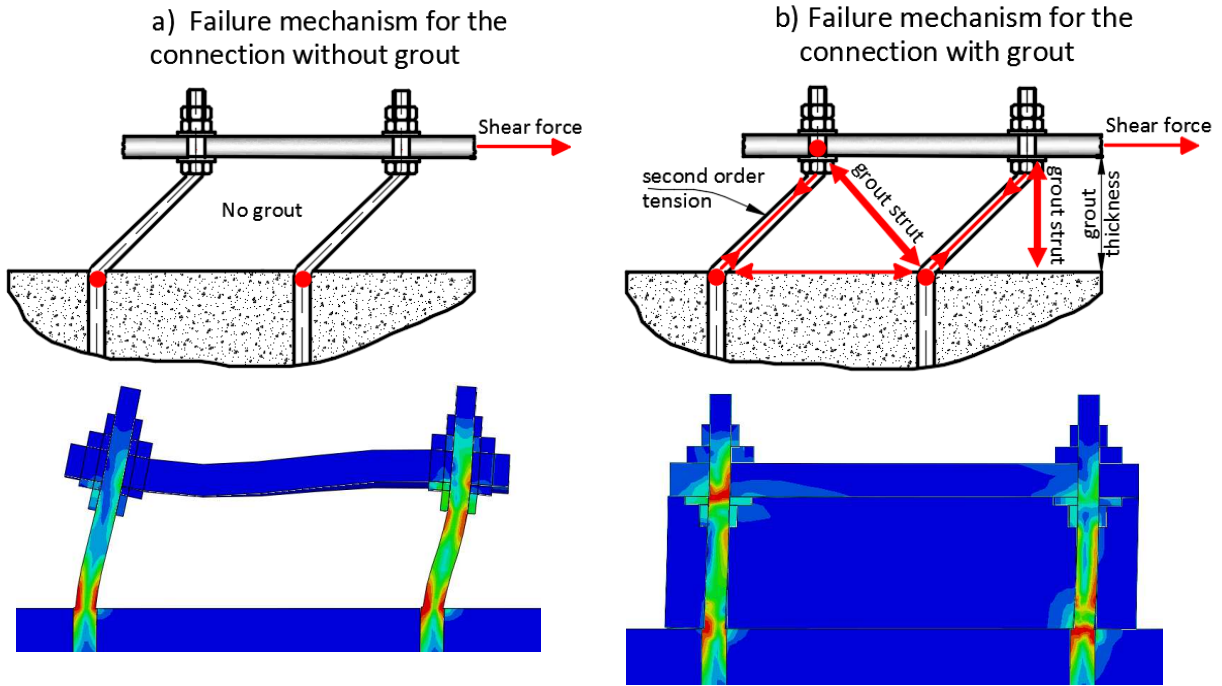
14

a) Failure mechanism for the connection without grout

b) Failure mechanism for the connection with grout

Fig. 18: Typical failure mechanism with and without grout
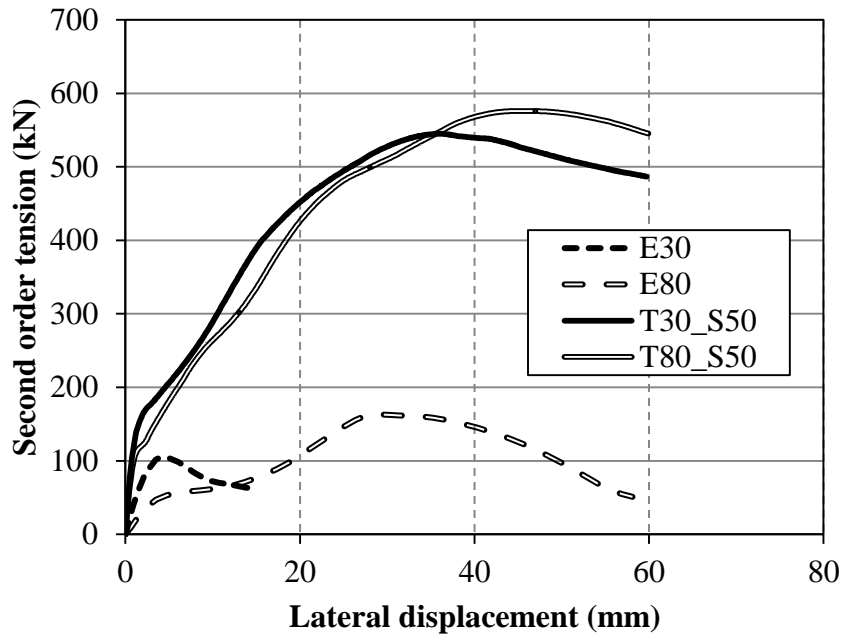
Fig. 19: Second order tension developed in anchor rods

9. Comparison between codes of practice and FE results

The shear strength calculated based on EC3 [11], European pre-standard CEN/TS4 [27] and ACI [28] was compared with the FE results as it is depicted in **Fig. 20**. The FE analyses were conducted taking into account that the concrete pedestal did not suffer major damages which alter the behaviour of the connection. This approach is frequently used in engineering practice by providing large edge distances between the concrete edge and anchor rod or by reinforcing the pedestal [3] to avoid concrete failure (e.g., concrete shear breakout). As a

15

consequence, the shear capacity calculated based on the regulations above mainly considers the steel failure. In other words, the concrete failure did not control the capacity of the connection.
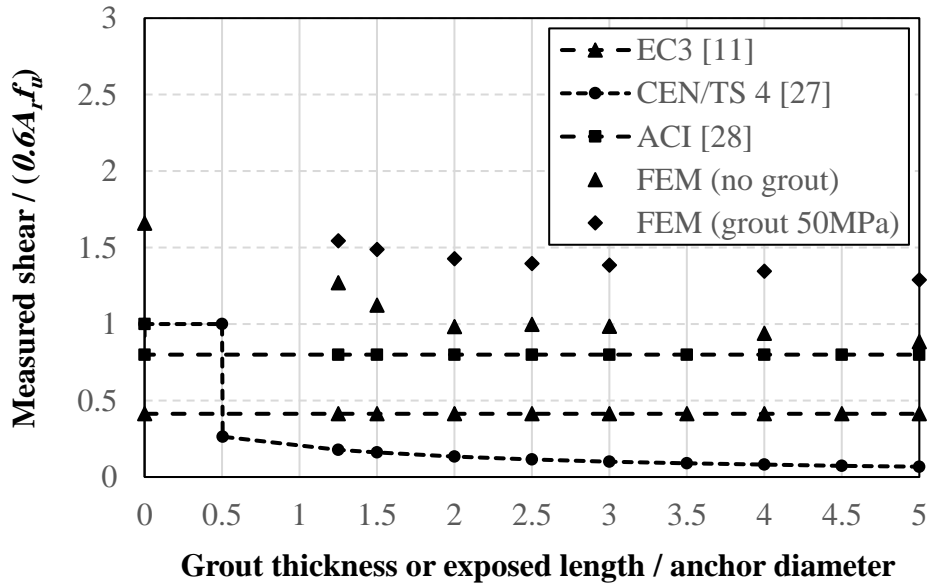
When the exposed length exceeded half of the anchor diameter, CEN/TS4 takes into account the effect of the exposed length by calculating the moment capacity of the anchor rod and hence the shear resistance. The calculated shear strength reduces with the increase of grout thickness; this trend was also observed by the FE analysis results. Nevertheless, CEN/TS4 does not consider the positive influence of grout (i.e., grout strut, friction and second order tension) which enhances the shear strength of the connection significantly, as it was observed earlier (see section 7 and **Fig. 16**). As a result, the values calculated by the CEN/TS4 were too conservative. For instance, the shear load obtained by the FE analyses was ranging between 2 and 20 times greater than the design value, for thin and thick grout, respectively. This was similar to what it was observed by COST/WG2 [29] that compared test results of the shear capacity of column base connections with the design value. The experimental values obtained were between 10 and 25 times greater than the design value. On the other hand, both ACI and EC3 regulations calculate the shear capacity independent of the exposed lengths of the anchor rod which leads to, unreasonably, the same shear strength for the different grout thickness. It is evident that the design shear values were calculated based on the connection with sole anchor rods. ACI is less conservative, particularly for the connection with large exposed length.

The significant discrepancy between the design values suggested by various codes of practice and the low predicted shear strength compared with the FE models, reveals that the behaviour of the base plate connection under shear force and different grout thickness is yet not fully understood and documented.

10. Mathematical modelling of column bases under shear load

The cited regulations and other studies [4,[30,[31] carried out to predict the shear capacity of the anchor rod have overlooked the deformation check despite that the captured lateral displacement was large and may violate the serviceability limit state. In this study, a mathematical equation defines the shear force, and corresponding lateral displacement is proposed.

The Component Method, which is the current state-of-the-art analytical technique to model the steel-concrete composite (SCC) behaviour will be utilised herein as it decomposes the SCC model into a set of individual basic components and it can be very benefial for out study. The mechanical properties (e.g., resistance, stiffness, and deformation capacity) of each component will be studied individually before being combined to define the mechanical properties of the overall SCC model. The use of the component method in the modelling of column base connections will give an accurate prediction of their behaviour [32-[34]. The component method will be employed for a derivative mathematical equation that predicts the column bases behaviour in shear.

10.1. Derivation of response in elastic range

Within the elastic limit, there were two major observations during the analysis. One is that the second order tension is relatively small comparing with the plastic range, thus the lateral displacement is mainly resisted by the bending resulted in the anchor rods. The second observation is that the initial stiffness of the connection was independent of the grout thickness and similar to the model when the exposed length is equal to zero. Therefore, the lateral stiffness of the anchor rods within the elastic range can be expressed as a cantilever beam with a lever arm equal to the thickness of the base plate, t_p, plus half the thickness of the anchor rod, d_r. Hence, the lateral stiffness K can be obtained from $K = 3EI/(t_p + d_r/2)^3$, where E and I are the modulus of elasticity and moment of inertia of the anchor rod, respectively. Consequently, the shear force (V_{el}) against the lateral displacement (u) in elastic range can be calculated using **Eq. (2)**.

$$V_{el} = n \frac{24EI}{(2t_p + d_r)^3} u \tag{2}$$

Where: I is the moment of inertia for anchor rod ($\pi d_r^4/64$) and n is the number of the anchor rods.

10.2. Derivation of response in plastic range

At large lateral displacements, the tension force on the anchor is increased rapidly. Due to the increase of the tension force in anchor rods, the bending capacity should be low, and it can be ignored. The shear force can be mainly resisted by the tension resulting in the anchor rods (second order tension), grout strut, and bearing between the rod and grout, as well as the friction between the base plate and grout.

The tension in the anchor will remain constant as it exceeded the elastic limit, and its magnitude is calculated using **Eq. (3)**. As it was observed in the analysis, the failure of the connection (shear, flexural-shear and tension failure) was different for various grout thicknesses. Also, the shear capacity was higher for the connection exhibited shear failure (connection with thin grout thickness). Therefore, coefficient α is proposed to account for this effect based on result observations and its value is 0.9, 0.85 and 0.8 for shear, flexural-shear and tension failure, respectively. The friction force changes with the lateral displacement since it relates to the vertical component of anchor rod tension and its value is given by **Eq. (4)**.

$$T = \alpha A_s f_u \tag{3}$$
$$F = T sin(\theta)\mu \tag{4}$$

Where: T is the plastic tension resulting in anchor rod due to the lateral displacement (N); f_u is the ultimate tensile strength of anchor rod (MPa); A_s is the instantaneous sectional are of the anchor rod will be discussed later in this section (see **Eq. (9)** in mm^2); F is the friction force between the base plate and the grout (N); μ is coefficient of friction; and α is a factor dependent on the mode failure (shear, flexural-shear and tension failure) and its value can be used as following:

1     $\alpha = 0.9$ for shear failure or $(t_g \leq d_r)$

2     $\alpha = 0.85$ for flexural-shear failure or $(d_r < t_g \leq 1.5d_r)$

3     $\alpha = 0.8$ for tension failure or $(1.5d_r < t_g)$.

4   The applied shear is in equilibrium with the horizontal component of the tension in the
5 anchor and the friction force between the base plate and grout. By applying the static
6 equilibrium equation, the applied shear is as follows:

$$V_{pl} = T\cos(\theta) + F \tag{5}$$

7   Substituting **Eq. (3)** and **(4)** into **Eq. (5)**, then:

$$V_{pl} = (\alpha A_s f_u)\cos(\theta) + (\alpha A_s f_u)\sin(\theta)\mu \tag{6}$$

$$V_{pl} = (\alpha A_s f_u)[\cos(\theta) + \sin(\theta)\mu] \tag{7}$$

8   From **Fig. 21** the value of $\cos(\theta) = u/L'_r$ and $\sin(\theta) = t_g/L'_r$ where: u is the lateral
9 displacement, t_g is the grout thickness, and L'_r is the deformed length. By substituting these
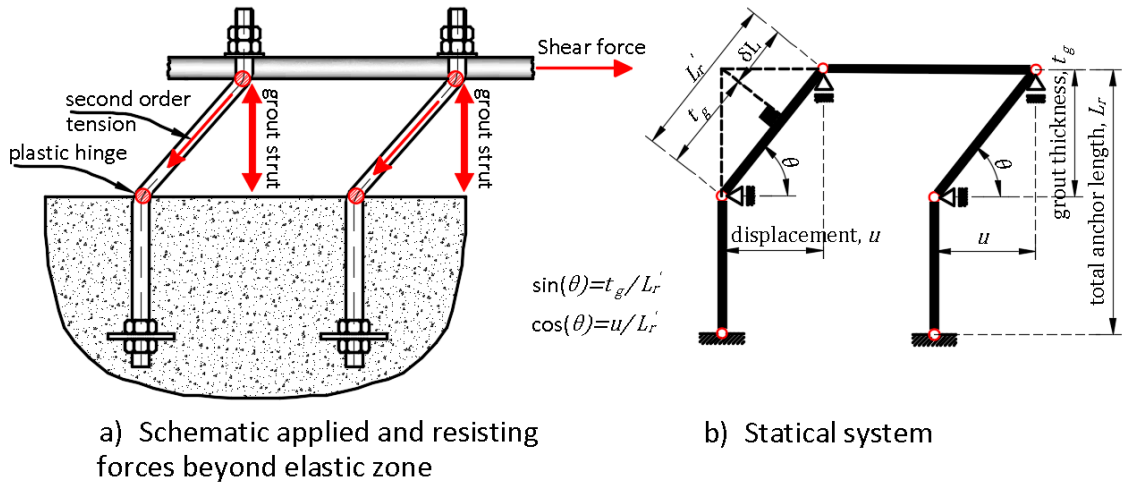10 values into **Eq. (7)**, then:

$$V_{pl} = (\alpha A_s f_u)\left[\frac{u}{L'_r} + \frac{t_g}{L'_r}\mu\right] \tag{8}$$

11   Since the anchor rod exhibits large lateral displacements under the applied shear force,
12 the effect of the reduced area should be taken into account. From the strength of material
13 theory, the deformation is assumed to occur at a constant volume (i.e., $[A_s L_r = A_r(L_r + \delta L)]$), then the instantaneous cross-section, A_s, is related to the initial cross-section, A_r, and
14 $\delta L)]$), then the instantaneous cross-section, A_s, is related to the initial cross-section, A_r, and
15 can be calculated using **Eq. (9)**.

$$A_s = \frac{A_r L_r}{L_r + \delta L} \tag{9}$$

$$\delta L = L'_r - t_g \tag{10}$$

16 Where: A_s is the instantaneous sectional are of the anchor rod (mm^2); A_r is the initial
17 sectional are of the anchor rod (mm^2); δL is the elongation of anchor rod (mm); L_r is the total
18 length of anchor rod from the top face of base plate to the anchor plate as it is shown in **Fig.
19 21** (mm).

20

a) Schematic applied and resisting   b) Statical system
     forces beyond elastic zone

21

22   **Fig. 21:** Schematic forces and static system

23

24   Substituting **Eq. (9)** and **(10)** into **Eq. (8)**, then the lateral displacement-shear force of the
25 connection in plastic range can be given as:

$$V_{pl} = n\frac{\alpha A_r L_r f_u}{L_r - t_g + \sqrt{u^2 + t_g^2}} * \frac{u + t_g\mu}{\sqrt{u^2 + t_g^2}} \tag{11}$$

Where: V_{pl} is the shear force in plastic zone (N); u is the corresponding lateral displacement (mm); n is the number of anchor rods; A_r is the initial sectional are of the anchor rod (mm^2); L_r is the total length of anchor rod from the top face of base plate to the anchor plate (mm); f_u is the ultimate tensile strength of anchor rod (MPa); t_g is the thickness of grout (mm); μ is the coefficient of friction; and α is a factor dependent on the mode failure (shear, flexural-shear and tension failure) and its value can be used as following:

α =0.9 for shear failure or $(t_g \leq d_r)$

α =0.85 for flexural-shear failure or $(d_r < t_g \leq 1.5d_r)$

α =0.8 for tension failure or $t_g > 1.5d_r$).

The displacement-shear force was defined for the elastic and plastic range, separately. The point of intersection of the curve in the elastic zone and the curve in the plastic zone should be defined. Thus, it is required to define the shear force and the corresponding lateral displacement that satisfies **Eq. (2)** and **(11)**. The lateral displacement at the intersection point can be found by setting the right-hand side of both equations as equal, hence:

$$n \frac{24EI}{(t_p + d_r)^3} u = n \frac{\alpha A_r L_r f_u}{L_r - t_g + \sqrt{u^2 + t_g^2}} * \frac{u + t_g \mu}{\sqrt{u^2 + t_g^2}} \tag{12}$$

$$u = \frac{\alpha A_r L_r f_u (u + t_g \mu)(2t_p + d_r)^3}{24EI \sqrt{u^2 + t_g^2} \left(L_r - t_g + \sqrt{u^2 + t_g^2} \right)} \tag{13}$$

Within the elastic limit, the lateral displacement is small compared to the thickness of the grout; therefore, $\sqrt{u^2 + t_g^2} = t_g$, then:

$$u = \frac{\alpha A_r f_u (u + t_g \mu)(2t_p + d_r)^3}{24EIt_g} \tag{14}$$

By arranging the **Eq. (14)**, the lateral displacement at intersection point can be found by:

$$u = \frac{t_g \mu}{\dfrac{24EIt_g}{\alpha A_r f_u (2t_p + d_r)^3} - 1} \tag{15}$$

11. Comparison between the proposed equation and FE models

To validate and demonstrate the analytical model, one of the FE model (T80_S50) was calculated in detail, and the results of the proposed equation were compared with the FE results (specimens with concrete grout). The following data was used:

Modulus of Elasticity, $E = 200,000 MPa$;

Ultimate tensile strength, $f_u = 1010 MPa$;

Anchor rod diameter, $d_r = 20mm$;

Length of the rod, $L_r = 625mm$;

Effective sectional area of the rod, $A_r = 208.57mm^2$;

Thickness of the base plate, $t_p = 25mm$;

Thickness of the grout, $t_g = 80mm$;

Coefficient of friction, $\mu = 0.45$;

Since $t_g > 1.5d_r$ the failure mode will be tension failure; hence, $\alpha = 0.8$.

$$I = \pi d_r^4 / 64 = \pi * \frac{(16.3)^4}{64} = 3463.38 mm^4$$

Firstly, the lateral displacement at the intersection point between the elastic and plastic limit is calculated using **Eq. (15).**

1
$$u = \frac{t_g \mu}{\dfrac{24EIt_g}{\alpha A_r f_u (2t_p + d_r)^3} - 1} = \frac{80 * 0.45}{\dfrac{24 * 200{,}000 * 3463.38 * 80}{0.8 * 208.57 * 1010 * (2 * 25 + 20)^3} - 1} = 1.635mm$$

2   The displacement at the intersection between the elastic and plastic curve is 1.635mm.
3 Therefore, **Eq. (3)** is valid for displacement less than 1.635mm, and **Eq. (11)** is valid for
4 displacement larger than the aforementioned value, then:

5
$$V_{el} = n \frac{24EI}{(2t_p + d_r)^3} u = 4 \cdot \frac{24 \cdot 200{,}000 \cdot 3463.38}{(2 \cdot 25 + 20)^3} u = 193.868u, \quad for \ u \leq 1.635mm$$

6
$$V_{pl} = n \frac{\alpha A_r L_r f_u}{L_r - t_g + \sqrt{u^2 + t_g^2}} \frac{u + t_g \mu}{\sqrt{u^2 + t_g^2}} = 4 \frac{0.8 \cdot 208.57 \cdot 625 \cdot 1010}{625 - 80 + \sqrt{u^2 + 80^2}} * \frac{u + 80 \cdot 0.45}{\sqrt{u^2 + 80^2}}$$

7
$$V_{pl} = \frac{421.31x10^6}{545 + \sqrt{u^2 + 80^2}} * \frac{u + 36}{\sqrt{u^2 + 80^2}} \qquad for \ u \geq 1.635mm$$

8   The comparison between the proposed equation and the result of FEM is illustrated in
9 **Fig. 22**. The proposed equation gives accurate results in both elastic and plastic stage for the
10 connection with different grout thickness.

11

12
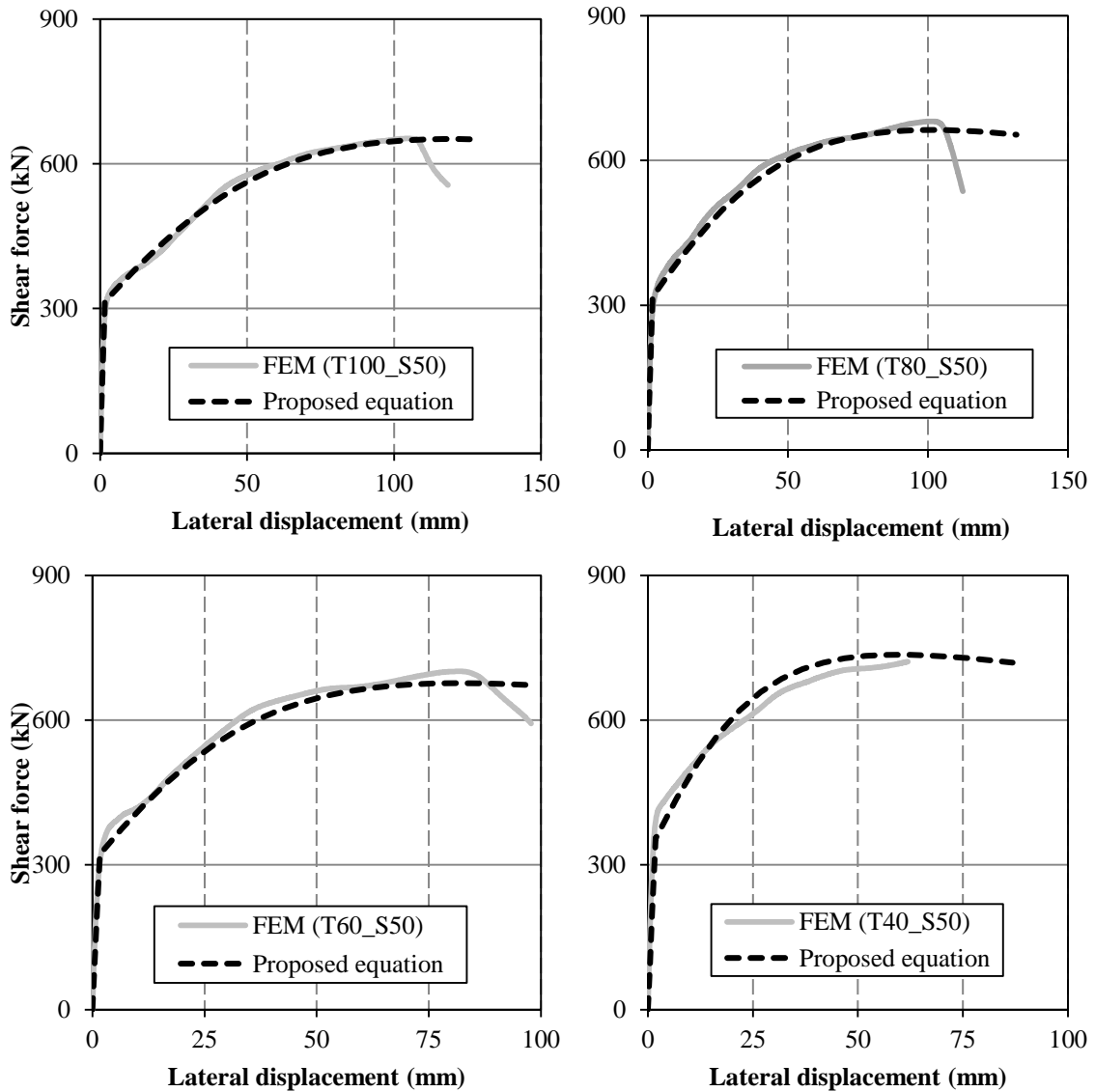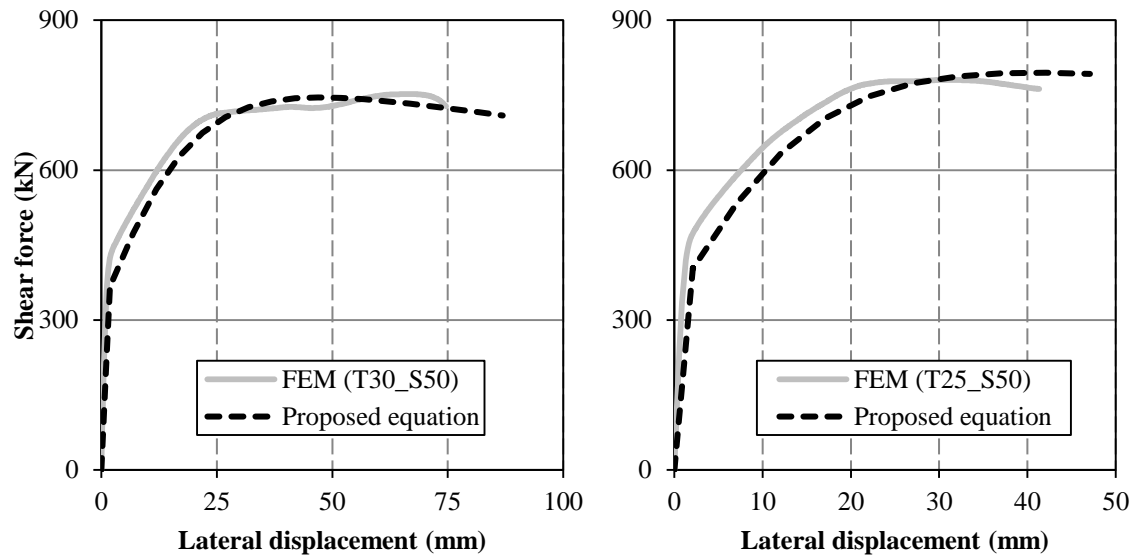
Fig. 22: Comparison between FE results and proposed equation

5. Concluding remarks

There is a lack of research which explores the effect of grout on the shear capacity of the base connection despite the fact that the grout layer is widely used in most base plate connections. In this paper, the shear capacity of the column base connections considering the thickness and strength of the cementitious non-shrink grout was investigated. The study was carried out employing comprehensive computational analyses on validated FE models (using ABAQUS v6.10), and the following observations were made.

With the increase of grout thickness, the shear capacity decreases and the ultimate displacement increases. However, the decrease in the shear capacity is not significant when different grout thickness is used. For example, the ultimate shear reduced by 10% when grout thickness was increased from 25mm to 50mm.

The behaviour of the connection improves when the effect of grout is considered. The grout increases the redundancy of the connection by developing grout struts and accordingly the number of plastic hinges required in the anchor rod for failure mechanism raises. This behaviour causes high tension to develop in the anchor rod of the connection with grout.

The forces resulting in the anchor rods under applied shear load are unequal which leads to the rotation of the front side of the base plate with a friction surface while the grout pad is stemmed although no axial force is applied. This friction force enhanced by the clamping action which arises due to the vertical component of the increasing tension force.

The grout enhances the shear capacity significantly by developing the grout strut and clamping action with the base plate. This positive influence overlooked in the aforementioned design codes of practice despite that the measured values revealed the improvement in capacity was between 20% and 40% when thin and thick grout layer was used, respectively.

The grout strength has a minor effect on the shear capacity of the connection, particularly when thin grout is used. For instance, the shear capacity decreased by only 4% when the

grout strength decreased from 50MPa to 6MPa. Therefore, the shear capacity can be calculated independently of the grout strength.

The lateral displacement under applied shear load is considerably high which may violate the serviceability limit state in certain cases or affect the forces in the steel column due to the second order effect. Nevertheless, the design codes check only the ultimate limit state and ignore the effect of this large lateral displacement on the forces developed in a connection's assemblages.

A mathematical equation is finally proposed which accounts for the shear capacity and lateral displacement. The comparison of the analytical curves with the corresponding FE results show that the equation is satisfactory for all examined models and can be used to check the strength and the serviceability limit state.

Acknowledgments

References

[1] Gomez, I., Kanvinde, A., Smith, C. and Deierlein, G., 2009. Shear transfer in exposed column base plates. AISC report, University of California, Davis & Stanford University.

[2] Grauvilardell, J.E., Lee, D., Hajjar, J.F. and Dexter, R.J., 2005. Synthesis of design, testing and analysis research on steel column base plate connections in high seismic zones. Structural engineering report no. ST-04-02. Minneapolis (MN): Department of Civil Engineering, University of Minnesota.

[3] Lin, Z., Zhao, J. and Petersen, D., 2013. Failure analysis of anchors in shear under simulated seismic loads. Engineering Failure Analysis, 31, pp. 59-67.

[4] Lin, Z., Petersen, D., Zhao, J. and Tian, Y., 2011. Simulation and design of exposed anchor bolts in shear. International Journal of Theoretical and Applied Multiscale Mechanics, 2(2), pp.111-129.

[5] Swirsky, R. A. 1977. "Lateral resistance of anchor bolts installed in concrete.".

[6] Nakashima, S. 1998. "Mechanical characteristics of exposed portions of anchor bolts in steel column bases under combined tension and shear." Journal of constructional steel research, 1(46), pp. 262-263.

[7] Gresnigt, A.M., Romeijn, A., Wald, F. and Steenhuis, C.M., 2008. Column bases in shear and normal force. HERON-ENGLISH EDITION-, 53(1/2), p.87.

[8] Petersen, D., Lin, Z., and Zhao, J., 2013. NEES-Anchor Final Report-Vol I - Cyclic Behavior of Single Headed Anchors. Submitted to National Science Foundation for the NEESR Project.

[9] ACI 351.1R-99. Grouting Between Foundations and Bases for Support of Equipment and Machinery.

[10] Guide, S.D., 2006. Base plate and anchor rod design. AISC, Chicago.

[11] EN, BS. "1-8. Eurocode 3: design provision of steel structures-Part 1-8: design of joints." British Standards Institution, UK (2005).

[12] Stark, J.W.B., 2011. Where structural steel and concrete meet. In Composite Construction in Steel and Concrete VI, pp. 406-418.

[13] Grout, Star Special. 110 by Five Star Products Inc. Fairfleld, CT. www. fivestarprociucts. com.

[14] Sika Corporation, based in Lyndhurst, NJ. Grouting & Quickset Mortars. www. usa.sika.com

[15] The steel construction Institute and The British constructional steelwork association 2011 Joint in steel construction: Simple joints to EC3. SCI/BCSA.

[16] Version, ABAQUS v6.10, 2010. User Documentation, Dassault Systems.

[17] Gomez, I.R., Kanvinde, A.M., John E. Bolander, Kenneth J. Loh. 2010. Behavior and Design of Column Base Connections. UMI 3427370.

[18] Delhomme, F., Debicki, G. and Chaib, Z., 2010. Experimental behaviour of anchor bolts under pullout and relaxation tests. Construction and Building Materials, 24(3), pp.266-274.

[19] Jaspart, J.P. and Vandegans, D., 1998. Application of the component method to column bases. Journal of constructional steel research, 48(2), pp. 89-106.

[20] Hsu, L.S. and Hsu, C.T., 1994. Complete stress—strain behaviour of high-strength concrete under compression. Magazine of Concrete Research, 46(169), pp.301-312.

[21] Hilleborg, A., "Stability problems in fracture mechanics testing", Fracture of concrete and rock edited by Shah, S. P., Swartz, S. E. and Barr, B., Elsevier Applied Science, 1989, pp. 369-378.

[22] Eurocode 2. Design of concrete structures – Part 1 – 1: General rules and rules for buildings Brussels: European Standards, CEN; 2003.

[23] Abaqus/CAE,"Abaqus/CAE Theory Manual", Abaqus Software, Ver. 6.10, Dassault Systemes Simulia Corp., Providence, Rhode Island.

[24] Kmiecik, P. and Kamiński, M., 2011. Modelling of reinforced concrete structures and composite structures with concrete strength degradation taken into consideration. Archives of civil and mechanical engineering, 11(3), pp.623-636.

[25] Petersen, D., Johnston, J., Zhao, J., Shahrooz, B. and Tong, X., 2013. Seismic Behavior and Design of Cast-In-Place Anchors. ACI Structure J, 110(1), pp. 53-62.

[26] Viest, I.M., 1956, April. Investigation of stud shear connectors for composite concrete and steel T-beams. In Journal Proceedings, 52(4), pp. 875-892.

[27] DD CEN/TS 1992-4:2009. Design of fastenings for use in concrete.

[28] ACI Committee 318, 2008. Building Code Requirements for Structural Concrete (ACI 318-02) and Commentary (ACI 318R-02), Farmington Hills, MI.

[29] Heron, 2008. Special issue: Steel column bases. Volume 53, issue 1/2, Delft.

[30] Alqedra, M.A. and Ashour, A.F., 2005. Prediction of shear capacity of single anchors located near a concrete edge using neural networks. Computers & structures, 83(28), pp. 2495-2502.

[31] Silva, John F., 2006. Anchorage in Concrete Construction. Ernst & Sohn, Berlin, Germany.

[32] Wald, F., Sokil, Z. and Jaspart, J.P., 2008. Base plate in bending and anchor bolts in tension. Heron, 53(1/2).

[33] Tsavdaridis, K.D., Shaheen, M.A., Baniotopoulos, C. and Salem, E., 2016. Analytical approach of anchor rod stiffness and steel base plate calculation under tension. Structures, (5), pp. 207-218.

[34] Wald, F., Steenhuis, C.M., Jaspart, J.P. and Brown, D., 2000. Component method for base plate. Journal of Constructional Steel Research, in printing.